


# Metastable effects on martensitic transformation in SMAs

## Part X. An approach to thermodynamic changes induced for the S-shaped cycles in thick wires of NiTi

V. Torra<sup>1</sup>  · F. Martorell<sup>1</sup> · Q. P. Sun<sup>2</sup> · A. Ahadi<sup>3,4</sup> · F. C. Lovey<sup>5</sup> · M. Sade<sup>5</sup>

Received: 1 March 2016 / Accepted: 1 October 2016 / Published online: 14 October 2016  
© Akadémiai Kiadó, Budapest, Hungary 2016

**Abstract** The transformation and retransformation paths realized at constant stress in wires of NiTi SMAs show a horizontal or “flat” behavior in the hysteretic cycle. After sinusoidal cycling at 0.01 Hz (i.e., training) with a maximal strain of 8 %, the thicker wires of NiTi SMAs, with a diameter of 2.46 mm, have the stress–strain cycles with one S-shaped behavior. A “similar” change appears by varying the grain sizes in the samples, i.e., from 80 to 20 nm. Furthermore, the local measurements of temperature suggest that cycling induces changes in the transformation mechanisms associated with the evolution from horizontal to S shape. For instance, the associated energy evolves from localized transformation to homogeneous heat production in S-shaped cycles. Thermodynamic analysis establishes a link between heat capacity and the slopes of the coexistence curve in  $f$ – $x$  or in  $\sigma$ – $\varepsilon$  via the  $(\partial\varepsilon/\partial\sigma)_{\text{coex}}$ . The flat cycles were coherent with the classical

latent heat, i.e., dissipation at constant stress. In the S-shaped cycles, the heat during the phase change seems redistributed as heat capacity against progressive stress. Preliminary direct measurements are coherent with the evolution of the  $(\partial\varepsilon/\partial\sigma)_{\text{coex}}$  against strain.

**Keywords** SMA · Martensitic transformation · S-shaped cycles · NiTi · Latent heat · Heat capacity · Thinner and thick wires · Grain size

### Introduction

Many physical systems show *phase transitions*. These are characterized by singularities in one of the thermodynamic potentials, such as free energy, and hence by discontinuities in their derivatives. The pioneer work of Ehrenfest [1] published in 1933 classified phase transitions according to whether the first, second, etc., derivative of the free energy

V. Torra: Retired from UPC (2012), Applied Physics Department, E-08034, Barcelona, Catalonia, Spain.

✉ V. Torra  
vtorra\_1@yahoo.com

F. Martorell  
ferranmc@gmail.com

Q. P. Sun  
meqpsun@ust.hk

A. Ahadi  
AHADI.Aslan@nims.go.jp

F. C. Lovey  
lovey@cab.cnea.gov.ar

M. Sade  
sade@cab.cnea.gov.ar

<sup>2</sup> Department of Mechanical and Aerospace Engineering, The Hong Kong University of Science and Technology, Clear Water Bay, Kowloon, Hong Kong, SAR, People’s Republic of China

<sup>3</sup> International Center for Young Scientist (ICYS), National Institute for Materials Science (NIMS), 1-2-1 Sengen, Tsukuba, Ibaraki 305-0047, Japan

<sup>4</sup> State Key Lab of Water Resources and Hydropower Engineering and School of Civil Engineering, Wuhan University, Wuhan, China

<sup>5</sup> Metal Physics Group, Centro Atómico de Bariloche, Instituto Balseiro and CONICET, 8400 Bariloche, RN, Argentina

<sup>1</sup> Personal Research Group (PRG), Villarroel 162, 08036 Catalonia, Barcelona, Spain

showed a discontinuity and called them, respectively, first-order, second-order, etc., transitions. As the first derivative of the relevant thermodynamic potential is discontinuous in the case of a first-order phase transition, such a phase transition will usually be accompanied by a latent heat. Currently, it is realized that not only discontinuities but also divergences at the phase transition point are important. All higher-order phase transitions are grouped together as *critical* or *continuous* phase transitions. The term “continuous” phase transition was introduced by Landau in their classic paper on the theory of phase transitions [2].

The martensitic transformation (MT) is the origin of the particular properties of shape memory alloys (SMAs). The MT was considered a solid–solid first-order phase transition with hysteresis between metastable phases. The SMAs are smart materials with a wide range of practical and potential applications. For instance, several applications are devoted to health solutions, e.g., in orthodontic applications, and their use was studied for dampers in civil engineering and for their actions in morphing. The experimental analysis of SMAs shows a hysteretic behavior in, for instance, stress–strain or strain–temperature representation. In fact, series of continuous cycles in stress–strain shows a monotonic SMA creep and a practical reduction in the available deformation associated with the cross section of the samples. In the temperature-induced transformations without external stresses, the interaction between martensite variants expands the transformation temperatures to more than 30 K. These interactions largely increase the difference between  $M_s$  (martensite start) and  $M_f$  (martensite finish). The asymptotic increase of creep in stress-induced transformations and the larger difference between  $M_s$  and  $M_f$  suggest some non-classical behavior in SMAs in comparison with conventional phase transitions with an extremely reduced temperature span. The alloy composition and the heat treatments establish the transformation behavior [3, 4].

In general, the MT was considered a “first-order” phase transition with latent heat that requires a constant stress in the transformation from parent to martensite. At the end of the 1980s [3], the appearance of “minor actions” as the intrinsic thermoelasticity and its associated pseudoelasticity in single crystals of CuAlZn suggests “difficulties” in the classical analysis of SMAs. For instance, the single interface measurements suggest some “minor” difficulties in the classical idea of a “first-order” transformation in the SMA. The studies devoted to damping of SMAs realized in NiTi for wires of 2.46 mm of diameter [5–10] establish the appearance of the S-shaped cycles, i.e., an inherent behavior without the flat cycles typical of thinner wires. The intrinsic S-slopes appear in the stress–strain representations without the thermal effects induced by cycling rate actions.

In recent years, the authors published a series of works in *JTAC* devoted to the mesoscopic properties of SMAs and their influence in SMA applications, in particular related to the metastability of the parent and martensite phases, under the title “Metastable effects on martensitic transformation in SMA” (papers I to IX in ref. 5). The authors’ series of recent papers focuses on temperature effects, strain aging [5, 6], and coupling with hysteretic behavior related to the grain size (GS) [11–16].

In this work, the study was devoted to the particular effects of S-shaped cycles, measuring simultaneously the local temperature in sinusoidal stress–strain cycles. Moreover, the measurements included a series of successive minor strain steps for local analysis. (See ref. [4], devoted to a review of the damping effects and to basic properties.)

The experimental measurements permitted a clear visualization of the sample evolution in cycling from “local” to “distributed” dissipation. Through thermodynamic parameters, the S-shaped cycles could be related to a particular behavior of the heat capacity. Using “larger” strain steps, the preliminary results showed a clear evolution of the dissipated heat against strain. In fact, the measurements suggest a probable change from the classical first-order transformation to an upper-order transformation. From the parent to martensite, the advancement of the transformation requires a progressive and relevant increase in the external stress. Deeper analysis of the heat capacity anomaly remains out of the limits of this paper. In fact, the actual state of the art suggests that direct calorimetric measurements are extremely difficult. The increased temperature span between  $M_s$  and  $M_f$  (i.e., between  $A_s$  and  $A_f$ ) related to interaction between martensite variants and other defects in a polycrystalline sample probably blur the effect of the S-shaped cycles obtained under stress.

In general, the two groups, i.e., Barcelona/Bariloche (BB) and Hong Kong (HK), undertook complementary experimental measurements focused on engineering applications (see references [3–10] for BB and [11–16] for HK). In this paper, we concentrate on the particularities of S-shaped cycles in thick wire. In fact, reduced diameters produce classical flat cycles, i.e., with standard first-order transition cycles. The observations synthesized in this paper suggest that the grain diameter seems to be the origin of changes from flat to S shape and, eventually, to an elastic behavior (Fig. 3-1).

## Experimental: materials and methods

In this case, the material mainly studied was acquired from standard furnishers. For instance, the use of SMAs in damping for stayed cables in bridges used SMA wires of

several meters in length. The dampers' preparation required the purchase of several hundreds of meters with reliable properties. Some sophisticated heat treatments appropriate for materials science laboratories using short samples remain completely out of the end user capability. In fact, a damper appropriate for cable no. 1, i.e., a stayed cable in a facility (ELSA)<sup>1</sup> used 4 m of one NiTi wire. Two wires of 1.25 m were used in damping the cable of IFST-TAR<sup>2</sup> (See ref. 4 and references therein).

For the BB group, we used a NiTi alloy in the pseudoelastic state, supplied in several orders and years (2007–2012) by Memry (CT, USA), a division of SAES Getters (Italy), and previously by Special Metals Corp. (2004–2007) (New Hartford, NY, USA). Wires of two diameters are studied in the straight superelastic state. In the A wires, the surface of the samples was finished in a light (gray) oxide surface with a diameter of 2.46 mm. For the B wires with a diameter of 0.5 mm, the surface was black oxide. According to the supplier's certificates, the A wires' temperatures are similar, i.e., 248/247 K and 243 K. The certificate of testing by the furnisher indicated that the nominal wire composition was 55.95 and 55.92 mass% of Ni balance Ti. The composition included other minor components, for instance, 270 ppm of C, 234 ppm of O, and reduced quantities (under 0.01 mass%) of more than 25 elements (Si, Cr, Co, Mo, W, Nb, Al, Ba, H, Fe, etc.). Some minor differences in composition were observed in the data sheets for the different orders. For instance, in the sheets, the repeatability was close to  $\pm 0.01$  mass% with similar A wires.

The stress–strain–temperature–time studies were also highly relevant. The study was conducted using a conventional MTS810 at room temperature (near 293 K) in an air-conditioned room. The MTS had a chamber that was constructed in-house to maintain moderate temperatures between the room temperature and up to 323 K. Simple protective structures made of plastic or cellulose shells were built for studies of the minor transformation steps to prevent and smooth parasitic actions in the temperature by the direct fan actions and the air-conditioning equipment. Two devices, Instron 5567 and Instron 1123, were used with two cooling–heating standard thermal chambers, the 3119-005 (203–523 K) and 3110, respectively. The equipment was selected to perform measurements at working temperatures between 240 and 373 K. The

equipment was also appropriate for determining the Clausius–Clapeyron coefficient (i.e., 6 MPa K<sup>-1</sup> for the A and B wires [10]) and to investigate seasonal effects. One stress–strain equipment computer controlled was fabricated in-house to study the slow cycles in longer (1 m) B wire samples at approximately room temperature (below 313 K). The microstructure of the A wire was observed by transmission electron microscopy. A Philips CM200 LaB<sub>6</sub> microscope was used. The observed structure of furnished and cycled samples was similar: complex with a greater quantity of grain boundaries, dislocations, and martensite. The results establish that the A wire was textured along the  $\langle 111 \rangle$  direction. The microstructure appears in the form of small grains and subgrains with a minimum size of about 80 nm. In addition, some precipitate of TiC and Ni<sub>3</sub>Ti<sub>2</sub> were observed [4].

In general, one or two K-thermocouples (using thinner Chromel and Alumel wires of OMEGA) were wrapped around the samples for local time–temperature analysis. Wrapping prevents local compositional changes and stress induced by spot welding but introduces supplementary noise and a “mean” reading associated with a practical length (2–4 mm) of the SMA wire by the wrapping. Using two thermocouples, two OMEGA MJC “zero-points” permits completely separated readings with satisfactory reproducibility and reduced noise. The experimental data include one systematic uncertainty close to 1 or 2 K, i.e., according to OMEGA specifications. Each K-signal was digitized by an independent DMM Agilent U1251A. Using a proprietary program, two DMMs' data were stored in a PC using independent USB ports with time-controlled readings at 0.1, 1, and 2 Hz or a maximum reading rate close to 6–7 readings/s. The maximal mean rate was related to the DMMs' digitizing and the available capabilities of the portable Hewlett Packard Compaq. The temperature measurements furnished representative data for cycling up to 2 Hz.

The study in the HK Laboratory focused on the preparation of different grain sizes. A commercial polycrystalline NiTi sheet was purchased from Nitinol Devices Company (alloy: SE508) with slightly Ni-rich composition (50.9 at%Ni–49.1 at%Ti). The as-received sheets were annealed at a temperature of 1073 K for 1 h in a furnace with flowing argon atmosphere and quenched in cold water. The sheets were cold-rolled to achieve 42 % thickness reduction in 15 consecutive passes to a final thickness of 1 mm. To achieve different grain size (GS) in the nanocrystalline regime, the cold-rolled (CR) sheets were annealed in a Nabotherm furnace according to two batches of heat treatments. For batch 1 (recovery and recrystallization annealing), the specimens were annealed at temperatures of 523, 573, 623, 673, 723, 773, 823, and 873 K for 45 min followed by water quenching. For batch 2 (recrystallization

<sup>1</sup> European Laboratory for Structural Assessment (ELSA) Unit located at the Ispra (Italy) is part of the Joint Research Center (JRC) of the European Union.

<sup>2</sup> IFSTTAR: Institut Français des Sciences et Technologies des Transports, de l'Aménagement et des Réseaux located at Bouguenais, France.

annealing), the specimens were annealed well above the recrystallization temperature (623 K) at 758 K for 2 min and 793 K for 2, 3, and 6 min followed by water quenching. The microstructure of the annealed sheets was studied at half thickness using high-resolution transmission electron microscopy (HRTEM-JEOL 2010F) after mechanical polishing, dimpling, and ion milling.

The average GS was measured from several sets of dark-field TEM images by counting at least 500 grains using “ImageJ” software from National Institutes of Health (USA). Latent heat release during transformation was characterized by in situ measurement of the specimen’s temperature oscillation in displacement-controlled cyclic loading/unloading tensile tests with an MTS 858 universal machine at a frequency of 0.05 Hz. Dog-bone tensile specimens (1 mm thickness, 1.3 mm width, and 17.3 mm gauge length) were cut along the rolling direction and were used for mechanical tests. To measure the hysteresis loop and the Clausius–Clapeyron coefficient ( $d\sigma/dT$ ), isothermal tensile tests at different constant temperatures were performed in a universal testing machine (UTM).

## Experimental: cycling in thick and thinner wires

Recent studies centered on damping of civil engineering show discrepancies in hysteretic behavior [4, 7, 8] for different diameters: thick wires (A samples) and thinner wires (B samples). Figures 1 and 2 visualize the particular behavior of the hysteretic cycles for the two diameters. After cycling the samples of 0.5 mm or, eventually, with minor diameter remain in a flat transformation, i.e., by a classical first-order transformation realized at constant stress. In the initial cycles, the transformation showed several steps associated with martensite nucleation. After training, the A samples, with a diameter of 2.46 mm, needed a progressive stress and transformed into S-shaped cycles. The practical effect of the cycling effect appeared clearly under external and moderate “winter” temperatures. At, for instance, 273 K (i.e., 0 °C), the zero stress line according to the Clausius–Clapeyron value (near 6 MPa/K [9]) goes up hysteresis cycles for 120 MPa or the cycle goes down for the same stress. The B wire (0.5 mm) could not retransform and remained in martensite. See the position of the abscissa line (i.e., dashed line in Fig. 2) at

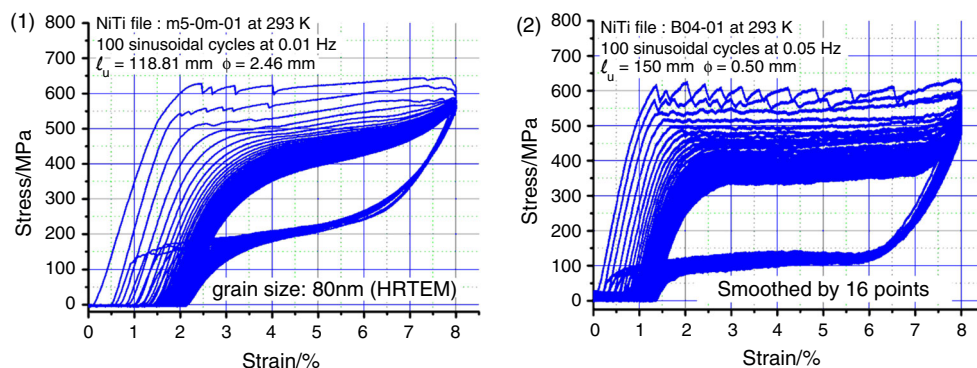


**Fig. 1** Progressive changes in cycling for the studied NiTi. **1** The “A” samples with a diameter of 2.46 mm. **2** The “B” samples with 0.5 mm of diameter

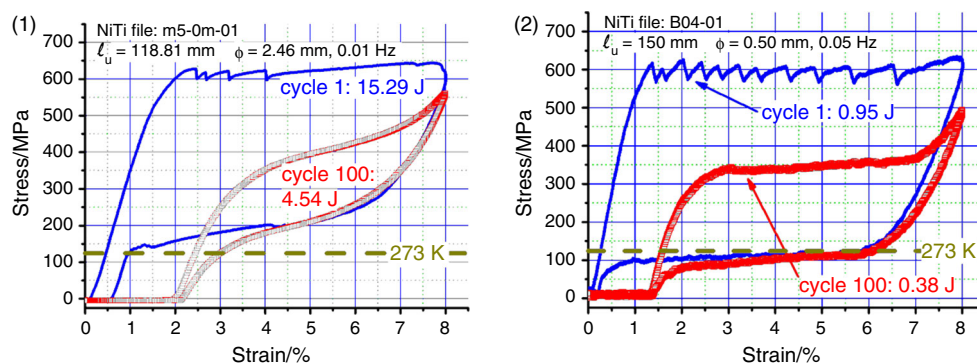


**Fig. 2** Cycles 1 and 100. The nucleation induces the steps in cycle 1. Dashed line: the base line position at 273 K stops completely the retransformation in the 0.5 wire. **1** After cycling, the cycle 100 was S-shaped. **2** After cycling, the cycle 100 remains flat

273 K. Figures 1-1 and 2-1 show sinusoidal cycles at 0.01 Hz, and Figs. 1-2 and 2-2 show sinusoidal cycles at 0.05 Hz. The frequency ratios agree with the radius ratio of the wires according to the requirements for similar losses by heat transfer in cylinders.

**Experimental: grain size study (HK Laboratory)**

Latent heat release during transformation was characterized by in situ measurement of the specimens’ temperature oscillation using cyclic loading/unloading tensile tests in displacement controlled by an MTS 858 universal machine. An ultra-thin K-type thermocouple with a diameter of 0.025 mm (and response time of 0.05 s) was taped to the specimen’s surface to capture the temperature evolution. Prior to the tests, the samples were trained at a low frequency (isothermal condition) to remove cyclic plasticity, i.e., the SMA creep. Figure 3-1 shows the isothermal stress–strain curves after training, i.e., after suppression of cyclic plasticity, at a frequency of 0.005 Hz. The figure shows that when the average grain size was reduced to below 60 nm, the stress–strain response showed a gradual smooth hardening. The pseudoelasticity and the hysteresis

loop area rapidly decreased and tended to vanish for an average grain size of 10 nm. Extended analysis of grain size (GS) effects established that the hysteretic behavior was progressively modified with the reduction in the grain size [11] due to a gradual change in the nature of phase transformation from a discontinuous first order to a continuous second order [14, 16]. Figure 3-2 shows that the steady-state temperature oscillation amplitude ( $\Delta T_{steady}$ ) decreases with grain size from 21.18 °C for an average grain size of 80 nm to 7.42 for an average grain size of 10 nm that permits an evaluation of the latent heat associated with GS (Fig. 4-1, 2). The dependence is clearly related to the grain size. In particular, it seems linear with the grain volume according to the linear representation visualized in Fig. 4-2.

The measurements of the HK group establish that the GS was situated between 64 and 27 nm for S-shaped cycles (Fig. 3-1). Flat cycles were situated near or over 80 nm. Previous HTEM measurements for diameter of 2.46 mm [4] suggest that the GS for the A wires was close to 80 nm using non-cycled samples (i.e., those with flat first cycle) coherent with the practical appearance of minor grains in cycled samples, probably induced by bands of the dislocation arrays and retained martensite created by the SMA

**Fig. 3** Grain size (GS) effects. (1) GS effects in the hysteretic behavior. (2) Amplitude of the steady-state temperature oscillations

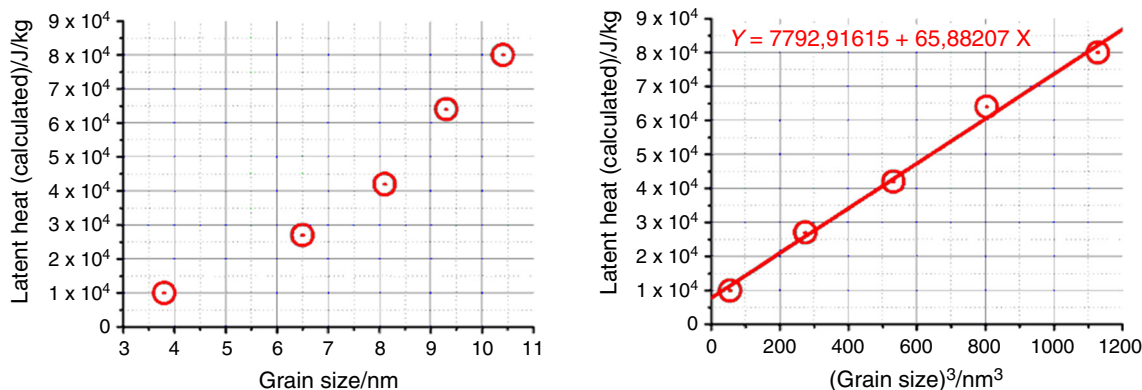
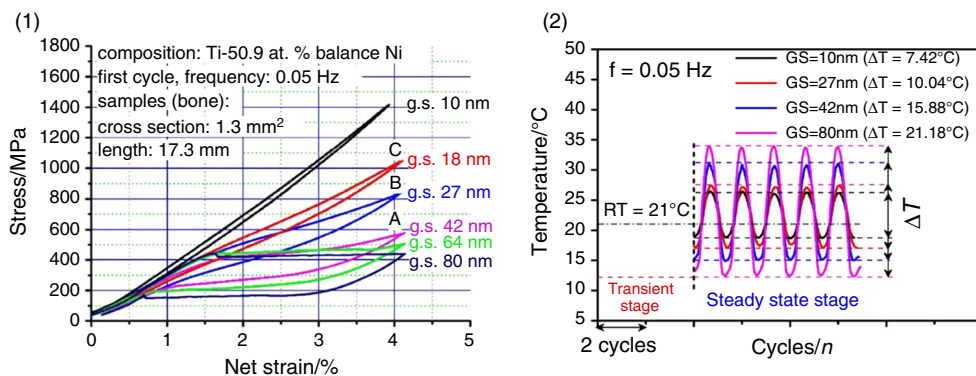


**Fig. 4** Dependence of the latent heat (L) against the grain size. 1 L against grain size. 2 L against volume size (data extracted from reference 15)

creep ( $>2\%$ ). The induced dislocations and retained martensite reduces, i.e., as a working hypothesis, the practical dimension of the grains [17]. On this basis, the B samples (their diameter remains out of our HRTEM possibilities) with lower SMA creep always show flat cycles that suggest an unchanged GS situated around 80 nm.

## Temperature effects on cycling

The wrapped K-thermocouples produce the temperature signals (Fig. 5) associated with the samples' training: 100 sinusoidal stress–strain cycles at 0.01 Hz (Fig. 5-1). In this case, the length of the SMA wire (type A) between the grips was 558 mm. The measurements establish some transitory effects in temperature. Figures 5-2 and 5-3 establish that the temperature oscillation was similar for two different positions in the NiTi wire: top (5-2) and bottom (5-3). The top position was at 86 mm of the upper grip, and the lower position was at 68 of the bottom grip. Rough visualization suggests that the temperature oscillation seems practically constant and independent of the creep actions. From a creep up to 2% (Fig. 5-1) and a maximal strain of 8%, the reduction in the transformed sample was a 25%. For instance, the net strain shrank from 8 to 6%.

Two actions were associated with the creep evolution on cycling. The first one was induced by several actions external to the samples. For instance:

- A. The fan action in the training cycles was especially relevant between cycles 1 and 100 for the A wires. The fan “on/off” action reduced/increased the maximal temperatures and modifies the shape of the hysteretic cycles and the dissipated energy [4].
- B. The minor differences between the span oscillation on top and bottom temperatures (i.e., 26 and 28 K) and the mean temperature value in Fig. 5-2, 3 were associated with the diameter of the air jet. In fact, the air jet from the fan could not cover completely the

upper part of the larger samples. In this sample, the length used was 558 mm between grips.

- C. The minor ripple of the temperature in the last part of Fig. 5-3 (i.e., between 5000 and 13,000 s) relates the external temperature wave induced by the start–stop of the conditioned air.

The evolution in temperature span cannot be considered a chimney effect. The cross section of the jet fan, if not completely including the length of the sample, induces an effective mixing of the surrounding air.

The second action was associated with an intrinsic evolution in the samples modifying the temperature oscillations. The increase in the creep progressively reduced the transformed mass and the oscillation amplitude of the local temperature. The reduction in the top temperature  $[(\Delta T_{\text{MAX}} - \Delta T_{\text{min}})/\Delta T_{\text{MAX}}]^{\text{top}}$  was 23.5%. Using the bottom temperature, which remains completely under the fan action, the temperature reduction  $[(\Delta T_{\text{MAX}} - \Delta T_{\text{min}})/\Delta T_{\text{MAX}}]^{\text{bottom}}$  was 9.6%. The difference between the “top” and “bottom” of the sample seems clearly affected by the cross section of the fan-jet actions on the lengthy samples.

A significant quantity of austenite disappeared progressively by cycling, i.e., 24% of the initially existing austenite could not transform. The results in Fig. 6 for the top (1) and bottom (2) include higher uncertainty in the link between the creep and the peak-to-peak temperature wave. The regression coefficients do not exceed 0.95 (0.93 and 0.86) and are affected by the transitory effects in heating and in cooling, the thermocouple wrapping and the sample movements, and the electrical noise and the air-conditioned temperature wave. The results suggest clearly that the reduction in the transformation by the creep was coherent with the transitory diminution in the temperature wave. In other words, as expected, the reduction in available transformed material reduced the latent heat effects.

Sinusoidal strain cycling produced “sinusoidal” temperature waves with minor delays associated with the

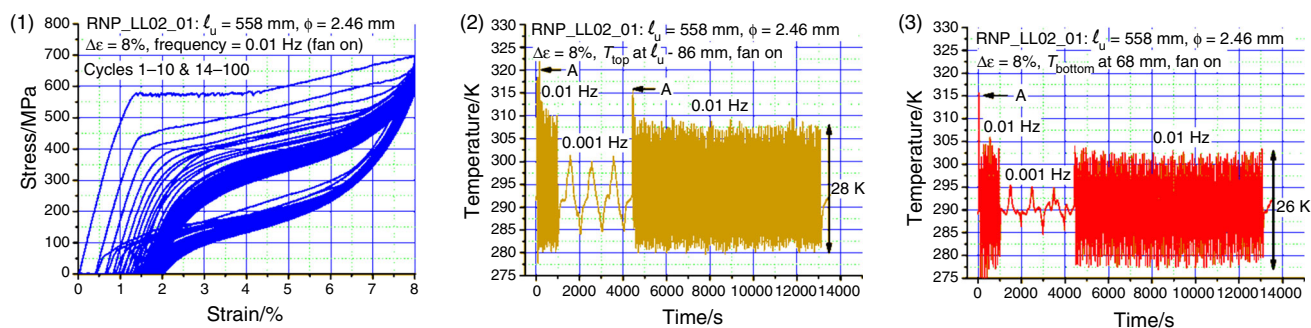


**Fig. 5** Hysteretic behavior and transitory effects in temperature: A: transitory or “starting” effects. **1** Sinusoidal cycles 1–10 and 14–100 in stress–strain at 0.01 Hz. **2** Temperature in the “top” position for

the cycles 1–100 at 0.01 and 11–13 at 0.001 Hz. ( $\Delta T$  close to 28 K). **3** Temperature oscillation in the bottom position close to 26 K

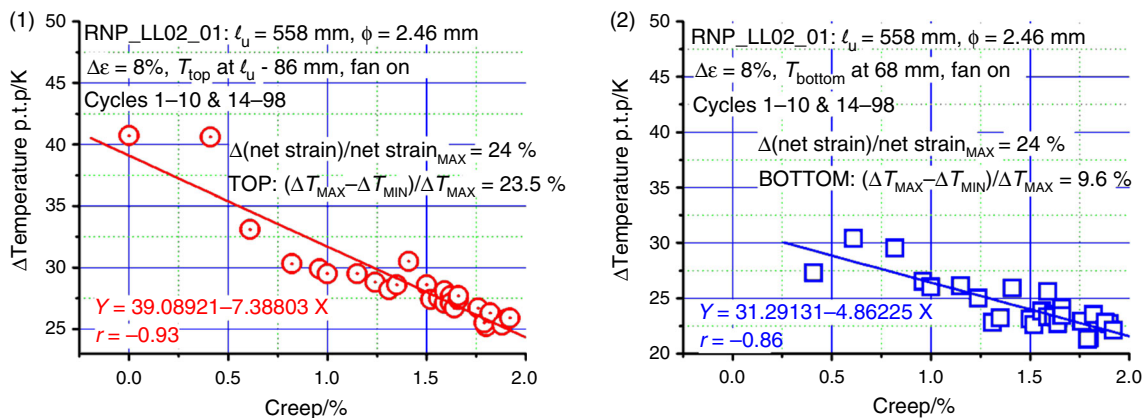


**Fig. 6** Peak-to-peak temperature wave and the creep increase. 1: Temperatures for the K-thermocouple in the top position. 2: Temperatures for the K-thermocouple in the bottom position

thermocouple position. From a sample “as furnished” with a length of 123.14 mm and a diameter of 2.46 mm, under a sinusoidal strain at 0.01 Hz, with a maximal deformation of 8 % and after 100 cycles, the S-shaped cycle starts practically at zero and ends near 600 MPa (Figs. 1-1, 2-1, 5-1). The results allow that, after cycling (i.e., 100 cycles of training), the transformation was modified in the NiTi wires from flat to S shape. The measurements suggest that the transformation process changed from local dissipation with a “transformation front” to a distributed transformation requiring progressive load (see below).

To improve the results, i.e., from local to distributed, the analysis was extended to cycles realized by strain steps. For instance, Fig. 7-1 shows cycle 1 in a representation in stress–strain coordinates. Figure 7-2 outlines the temperatures against the time for top (M) and bottom (B) thermocouples. Each “step strain” of 200 s was realized in two parts. In the first 4 s the strain increased “suddenly” and later, the next 196 s of a complete stop permitted a recovery of the thermal signal. The first cycles showed higher peaks of temperature induced when the “local”

transformations appeared in the position of each K-thermocouple. The conditioned air induced minor ripples (Fig. 7-2) between 5000 and 13,000 s. In fact, the first cycle showed a flat transformation (the first cycle in Figs. 1-1 and 5-1 corresponds to two lengths: 118 and 558 mm, respectively).

Cycling induces an increase in the creep. In cycle 107 (Fig. 8-1) the creep was 1.7 % with a reduction in the force steps and of the hysteresis width (compare Fig. 7-1 with Fig. 8-1). Figure 7-2 for cycle 1, in comparison with Fig. 8-2 (for cycle 107), shows one “homogenization” of the associate temperature steps in all parts of the sample. The transformation passes from local (i.e., a progressive displacement of the parent to martensite interface induced by the strain) visualized separately in the two thermocouples (Fig. 7-2) to a distributed transformation, i.e., a simultaneous transformation in the “complete” sample. Figure 9-1 shows partial cycles in a trained sample with a net deformation of 1.62 % cycling at 2 Hz. The amplitude of the temperature oscillation is similar for each K-thermocouple position (i.e., in the bottom and top of the

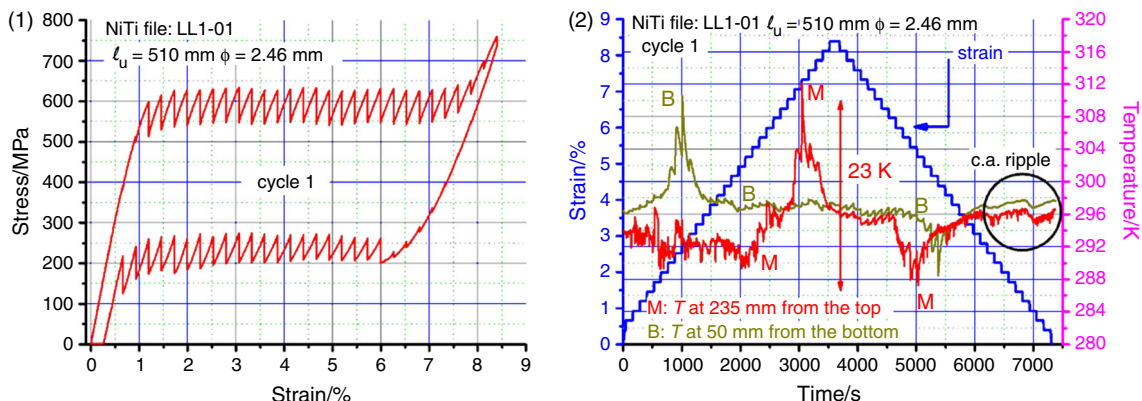


**Fig. 7** Strain steps effect on the hysteretic behavior for the cycle 1 with localized transformation. 1: Stress against strain. 2: Associated temperatures against time for top thermocouple (A) and bottom (B)

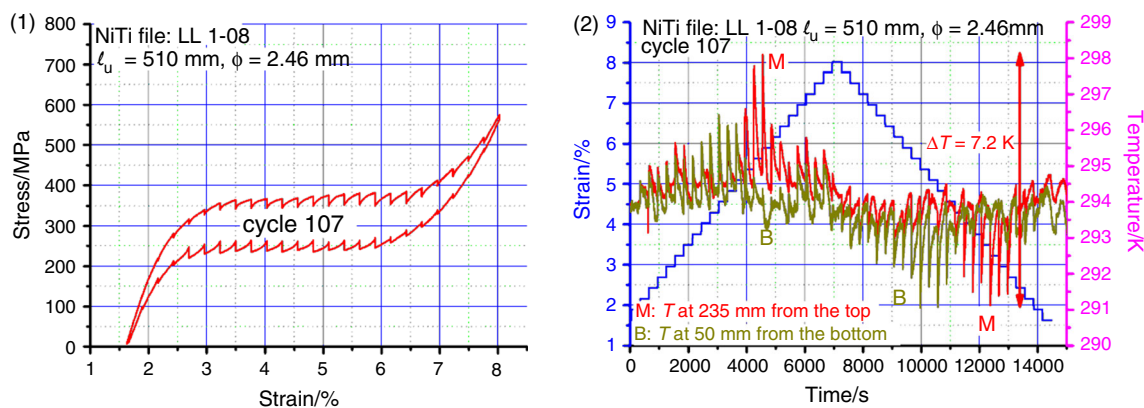


**Fig. 8** Behavior of the cycle 107 in strain steps with distributed transformation. 1: Stress against strain. 2: Associated temperatures against time for top thermocouple (A) and bottom (B)

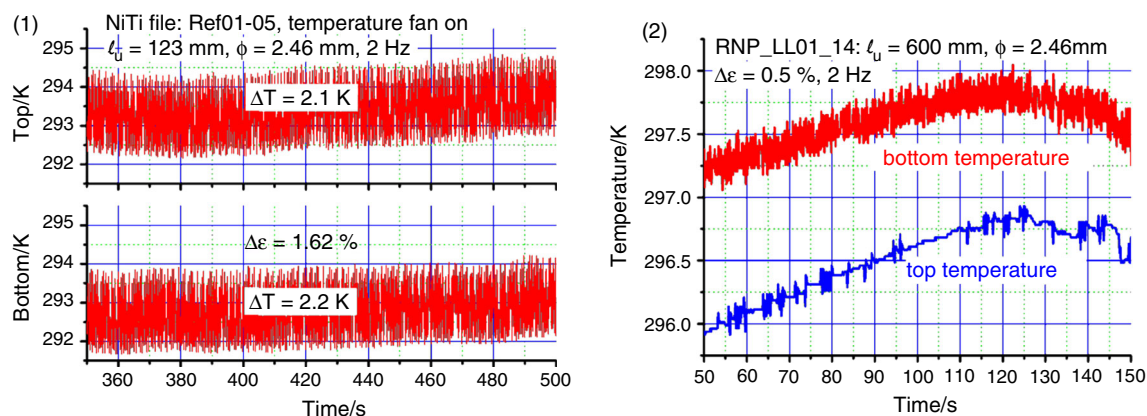


**Fig. 9** Temperature against time for a wire of 2.46 mm of diameter and reduced strains. 1: Strain of 1.6 % the temperature wave with the “same” amplitude in top and bottom of the wire. 2: Strain of 0.5 %.

sample), establishing that a minor transformation was realized simultaneously in the complete sample.

For reduced deformations (i.e., close to 0.5 %) the progressive strain process seems inhomogeneous. Part of the sample only activates elastic parts without dissipation. In fact, it seems that the sample realizes “simultaneously” minor transformations and also elastic processes (Fig. 9-2) for the bottom thermocouple (dissipation) and for the top thermocouple, i.e., in this case, the temperature oscillation was irrelevant in the top of the sample.

### Thermodynamic approach: the Clausius–Clapeyron equation

This section uses the notation and thermodynamics reasoning from a classical book, *Elements of Thermodynamics* [18], a graduate-level book that establishes in 160 pages an

The temperature wave shows dissipation in “bottom” and elastic behavior in “top” of the sample

interesting approach to thermodynamics for physicists. Consider that a 1-D system is a wire or a thinner cylinder with a cross section  $S^*$ . Under progressive external stress, the material experiences a first-order phase transformation equivalent to one MT, and the material converts progressively from parent (austenite) to martensite under an external force  $f_{\text{ext}(p \rightarrow m)}$ , increasing in length from  $x_p$  to  $x_m$  with an increase of  $\Delta x$  ( $\Delta x = x_m - x_p$ ). In general, the maximal increase in a crystallographic transformation of a single crystal can be considered around a 10 % (i.e., an associate strain of  $\varepsilon = 100 \Delta x/x_p \approx 10 \%$ ). In equilibrium, the external and internal forces compensate (Eq. 1). Neglecting the eventual change of the diameter and the associated external pressure effects, the surroundings realize work on the system  $\Sigma$  when the sample length increases by  $d\vec{x}$ . The external work on the system was A in Eq. 2, and, in quasi-static equilibrium, the external and internal (sample) forces compensate:



$$\vec{f}_{\text{ext}} + \vec{f}_{\text{int}} = 0 \tag{1}$$

$$W_{\text{ext} \rightarrow \text{sys}} = \int_A \vec{f}_{\text{ext}} d\vec{x} \tag{2}$$

The work realized by the system was B in Eq. 3 and, introducing stress ( $\sigma$ ) and strain ( $\epsilon$ ), the work was C in Eq. 4:

$$W_{\text{sys} \rightarrow \text{ext}} = -W_{\text{sys} \rightarrow \text{ext}} = - \int_B \vec{f}_{\text{ext}} d\vec{x} = -V \int_C \sigma d\epsilon \tag{3}$$

Quasi-static process relates extremely slowly ideal processes with the material describing the state equation. Reversible transformation requires that the external force ( $f_{\text{ext}}$ ) always remain equal to the internal force (permanent compensation between them). For instance, in a hydrostatic system, the external and the inner pressure remain strictly equal, i.e.,  $p_{\text{ext}} = p$  or, for a 1-D wire, the external force (outwards) compensates for the internal force induced by the transformation.

The coexistence effects in a 1-D wire as in a martensitic transformation usually considered as first-order establish that under an external force, the parent phase converts progressively in martensite by an increase in its length (from  $x_p$  to  $x_m$ ) and dissipates a latent heat (1–2 in Fig. 10-1). In the retransformation, the experimental force was reduced by the action of the hysteresis, and the length changed from  $x_m$  to  $x_p$  with one heat absorption. Figure 10 outlines an elementary working cycle 1–2–3–4. In the path 1–2, under the external force, the material converts to martensite, dissipating the latent heat and the entropy pass from  $S_p$  to  $S_m$ . The action of a minor force ( $df$ ) and temperature reduction ( $dT$ ) the elementary cycle describes the path 2–3. Later in 3–4 the retransformation recovers the parent phase: Minor increases in  $f$  ( $df$ ) and

$T$  ( $dT$ ) close the elementary cycles in the  $f$ - $x$  representation (similar to Clapeyron coordinates) and in the TS representation. For  $f$ - $x$  coordinates the area was the associated work and for TS coordinates, it was the associated heat.

The work equals heat and the balance reads as follows:

$$W_{\text{work realized}} = df_{\text{coex}}(x_m - x_p) = Q_{\text{absorbed}} = dT_{\text{coex}}(S_p - S_m) \tag{4}$$

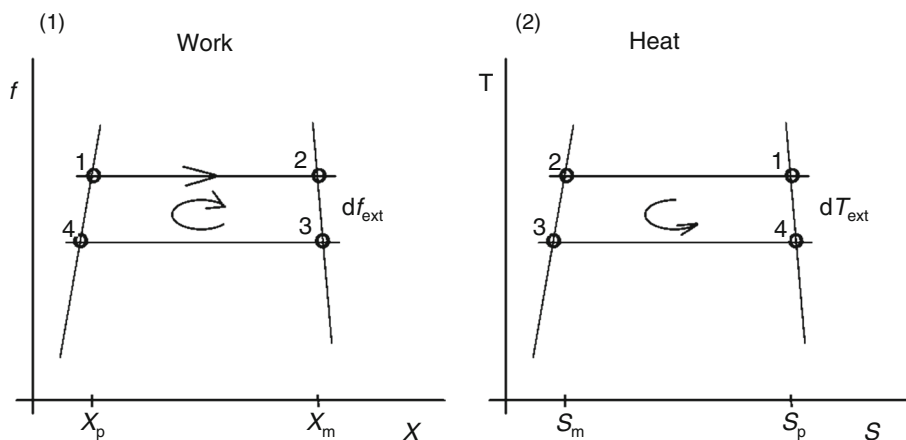
From (4) the Clausius–Clapeyron equation reads as follows:

$$\left( \frac{df_{\text{coex}}}{dT_{\text{coex}}} \right) = \frac{S_p - S_m}{x_m - x_p} = \frac{l_{\text{latent heat}(p \rightarrow m)}}{T(x_m - x_p)} \tag{5}$$

The value of Clausius–Clapeyron coefficient can be measured from series of working cycles at different temperatures. For CuZnAl a value of 1 MPa/K (3) was encountered; for CuAlBe, it was 2.2 (9); for CuAlNi, it was 1 MPa/K; and for the parent to hexagonal, it was 2 MPa/K [19, 20]. For NiTi values close to 6 or 6.3 MPa/K were indicated [4, 13].

The Clausius–Clapeyron equation relates a first-order phase transition with a flat process in the transition (i.e., at constant force and temperature), as, for instance, visualized in Fig. 1-2 for B wires. The situation for the hysteresis cycles of A wires in NiTi studied in this paper was completely different. The hysteresis cycles established a continuous increase of force (the S-shaped cycles) associated with the transformation (Figs. 11-1, 2-1, 5-1). Only using thinner wires (i.e., 0.5 mm in diameter or less), the hysteretic behavior remained flat and the transformation could be considered always as first order. In fact, Fig. 11-2 shows the representation of  $(d\epsilon/d\sigma)_{\text{coex}}$  against the net strain in the transformation parts of the hysteresis cycles outlined in Fig. 12-1.

**Fig. 10** Elementary cycles in quasi-static 1-D phase transition. The realized work in  $f$ - $x$  was equal to the heat dissipated in the TS representation. In the  $df_{\text{ext}}$  and the  $dT_{\text{ext}}$  the material remains in the phase coexistence



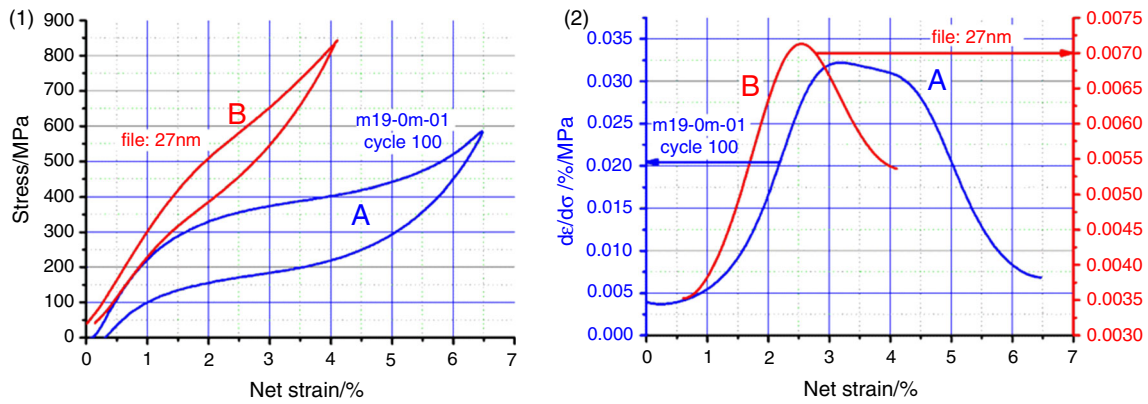


**Fig. 11** From S-shaped hysteretic behavior to some heat capacity anomalies. (1): Stress against net strain for the cycle 100 (sample of 2.46 mm up to 8 % (A) and the cycle 1 for grain size of 27 nm up to

4 % (B). (2): The values of  $d\epsilon/d\sigma$  against deformation corresponding to the same A and B curves of (1)

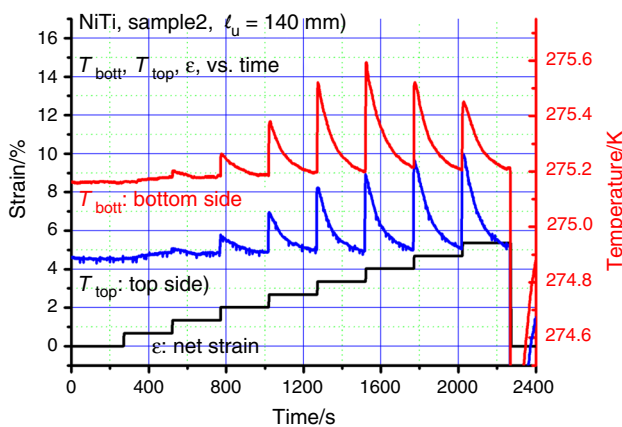


**Fig. 12** Strain and temperature for one stepped cycles. Using a cycled sample with a diameter of 2.46 mm the material was submitted to a series of equal strain steps separated by pauses. The associate temperature measurement against time was similar for two K-thermocouples situated in top and bottom of the sample

### A thermodynamic approach to $(d\epsilon/d\sigma)_{\text{coex}}$ in S-shaped cycles

The thermodynamic identity (first and second law) for one hydrostatic work [18] reads as follows:

$$\delta Q = TdS = dU + \delta W = dU + pdV \quad (6)$$

For a work in a wire, the thermodynamic identity of the hydrostatic system transforms as follows:

$$\begin{aligned} \delta Q &= TdS = dU - f dx = \left(\frac{\partial U}{\partial T}\right)_x dT + \left(\frac{\partial U}{\partial x}\right)_T dx - f dx \\ &= C_x dT + \left(T \left(\frac{\partial f}{\partial T}\right)_x - f\right) dx \end{aligned} \quad (7)$$

In a phase coexistence with one S-shaped transformation without a flat process, i.e., with a heat capacity  $C_{\text{coex}}$ , Eq. 7 reads as follows:

$$\partial Q_{\text{coex}} = C_{\text{coex}} dT_{\text{coex}} = C_x dT_{\text{coex}} + \left(T \left(\frac{\partial f}{\partial T}\right)_x - f\right) dx_{\text{coex}} \quad (8)$$

Dividing Eq. (8) by  $dT_{\text{coex}}$  and using  $dx/dT = (dx/df)(df/dT)$ , the heat capacity in the coexistence reads as follows:

$$\begin{aligned} C_{\text{coex}} &= \left(C_x + T \left(\frac{\partial f}{\partial T}\right)_x - f\right) \frac{dx_{\text{coex}}}{dT_{\text{coex}}} \\ &= \left(C_x + T \left(\frac{\partial f}{\partial T}\right)_x - f\right) \frac{dx_{\text{coex}}}{df_{\text{coex}}} \frac{df_{\text{coex}}}{dT_{\text{coex}}} \end{aligned} \quad (9)$$

The term  $(df/dT)_{\text{coex}}$  is the Clausius–Clapeyron coefficient, and roughly the previous equation for  $f$ ,  $x$ , or  $\sigma$  ( $\sigma = f/S^*$ ) and  $\epsilon$  ( $\epsilon = x_{\text{coex}}/x_p$ ) reads as follows:

$$C_{\text{coex}} = A \frac{dx_{\text{coex}}}{df_{\text{coex}}} = B \left(\frac{d\epsilon}{d\sigma}\right)_{\text{coex}} \quad (10)$$

Different series of measurements were performed to visualize the heat capacity change with strain. First, a series of partial cycles with the same strain was highly affected by the dissipation associated with hysteresis. A second series used steps of strain and associated pauses to homogenize the temperatures (Fig. 12). In cycled samples, up to 8 %, usually appeared in one SMA creep of 2 %, and the available net deformation does not exceed 6 %. The steps show a particular evolution of the temperature peaks. In Fig. 13 the evolution of the temperature peak against the associated strain was similar to the evolution of  $(dx/df)_{\text{coex}}$ .

### Conclusion and remarks

An analysis of the measurements suggests that the S-shaped measurements avoid the classical consideration of the MT as a first-order phase transition. For NiTi,

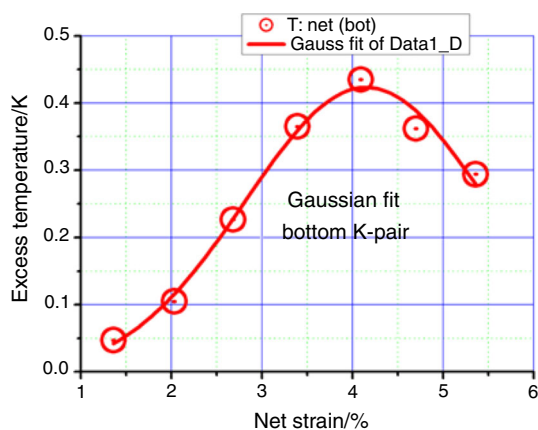


**Fig. 13** Evolution of the temperature peak value against the associate strain

cycling induces this particular behavior for relatively thick diameters. The thermodynamics associated with the Clausius–Clapeyron equation requires flat transformations (at constant force or stress and temperature) and for S-shaped cycles suggests a link between the  $(dx/df)_{\text{coex}}$  and the specific heat. In this frame the experimental temperature peaks associated with strain steps suggest an anomaly at a specific heat. More direct studies remain outside the interest of the authors. Particular behaviors of SMAs are relatively frequent in the studied alloys: stabilization in CuZnAl, the appearance of two phases in temperature-induced transformations in CuAlNi, dynamic effects in CuZnAl and CuAlBe, and grain size effects in NiTi [11, 13–16]. The results of this paper suggest that in cycled thick wires (2.48 mm in diameter), with an initial GS near 80 nm after series of working cycles, the dislocations’ arrays and retained martensite practically reduce the grain size to near 27 nm, and the initial flat first-order transition is converted into an S-shaped cycles with an upper-order phase transition.

The phase transition describes collective effects between the atoms. The progressive reduction in latent heat is coherent with the reduction in GS. The evolution from flat to elastic seems associated with a reduction of the available material and related to a reduction of GS. The appearance of S-shaped cycles can be estimated by the creep increase with an associated reduction of the flat part that reduces to an inflection point. In other words, the S-shaped transformation establishes a link between the previous elastic parent and the later elastic martensite. The progressive conversion from flat to S shape and later to “elastic” associated with a reduction of GS requires further and deep structural study.

The evolution from flat to S-shaped transformations relates a change from “local” to “distributed” dissipation of the NiTi 2.46 mm in diameter. In fact, the transformation

in the initial cycles shows local dissipation associated with progressive displacement of the interface parent to martensite, i.e., by latent heat dissipation (Fig. 7-2). After a series of working cycles, the dissipation appears simultaneously in all positions, as a distributed dissipation similar to one heat capacity (Figs. 8-2, 9-1). Only by extremely minor displacements, i.e., by strains close or under 0.5 %, the effect is reduced to mixed phenomena: elastic and minor dissipation (Fig. 9-2). A short thermodynamic overview of the phase transition associated with S-shaped hysteresis permits an estimation of the effect in terms of heat capacity (i.e., the specific heat).

If civil engineering uses dampers with SMA wires of “several meters,” the authors use standard furnishers for the acquisition of NiTi. Two furnishers of NiTi were used, the MEMRY (i.e., SAES Getters) for the BB Laboratory and Nitinol Devices Co. for the HK Laboratory.

**Acknowledgements** The authors wish to acknowledge Pablo Riquelme of CAB and Michele Vece of Pavia for their support with  $\sigma$ ,  $\varepsilon$ ,  $T$ , and  $t$  measurements. The paper was started with Guillem Carreras Diaz, MS (physics), who died on October 29, 2014. He was a colleague and friend of V.T. in the 1970s in the Thermodynamics Department at the University of Barcelona and also in the secondary school situated in Cornellà de Llobregat up to 1975. The common work was restarted in 2006 until Guillem’s death. His critical analysis of the measurements and formalisms and their extraordinary working capability remains forever an example for friends and colleagues.

## References

1. Ehrenfest P. Phase changes in the ordinary and extended sense classified according to the corresponding singularities of the thermodynamic potential. *Proc Acad Sci Amsterdam*. 1933;36:153–7.
2. Landau LD. Zur Theorie der phasenumwandlungen II. *Phys Z Sowjetunion*. 1937;11:26–35.
3. Lovey FC, Torra V. Shape memory in Cu-based alloys: phenomenological behavior at the mesoscale level and interaction of martensitic transformation with structural defects in Cu–Zn–Al. *Prog Mater Sci*. 1999;44–3:189–289.
4. Torra V, Isalgue A, Lovey FC, Sade M. Shape memory alloys as an effective tool to damp oscillations. Study of the fundamental parameters required to guarantee technological applications. *J Therm Anal Cal*. 2015;119(3):1475–533.
5. Torra V, Auguet C, Isalgue A, Carreras G, Lovey FC. Metastable effects on martensitic transformation in SMA Part IX. Static aging for morphing by temperature and stress. *J Therm Anal Calorim*. 2013;112:777–80.
6. Torra V, Carreras G, Lovey FC. Effects of strain aging at 373 K in wires of NiTi shape memory alloy. *Can Metall Q*. 2015;54–1:77–84.
7. Torra V, Auguet C, Isalgue A, Carreras G, Terriault P, Lovey FC. Built in dampers for stayed cables in bridges via SMA. The SMARTeR-ESF project: a mesoscopic and macroscopic experimental analysis with numerical simulations. *Eng Struct*. 2013;49:43–57.
8. Torra V, Carreras G, Casciati S, Terriault P. On the NiTi wires in dampers for stayed cables. *Smart Struct Syst*. 2014;13–3:353–74.

9. Isalgue A, Torra V, Yawny A, Lovey FC. Metastable effects on martensitic transformation in SMA Part VI. The Clausius-Clapeyron relationship. *J Therm Anal Calorim.* 2008;91(3):991–8.
10. Torra V, Carreras G, Casciati S, Terriault P. On the NiTi wires in dampers for stayed cables. *Smart Struct Syst.* 2014;13(3):353–74.
11. Ahadi A, Sun QP. Effects of grain size on the rate-dependent thermomechanical responses of nanostructured superelastic NiTi. *Acta Mater.* 2014;76:186–97.
12. Yin H, He Y, Sun QP. Effect of deformation frequency on temperature and stress oscillations in cyclic phase transition of NiTi shape memory alloy. *J Mech Phys Solids.* 2014;67:100–28.
13. Ahadi A, Sun QP. Stress hysteresis and temperature dependence of phase transition stress in nanostructured NiTi—effects of grain size. *App Phys Lett.* 2013;103:021902. doi:[10.1063/1.4812643](https://doi.org/10.1063/1.4812643).
14. Ahadi A, Sun QP. Stress-induced nanoscale phase transition in superelastic NiTi by in situ X-ray diffraction. *Acta Mater.* 2015;90:272–81.
15. Sun QP, Ahadi A, Li MP, Chen MX. Effects of grain size on phase transition behavior of nanocrystalline shape memory alloys. *Sci China Technol Sci.* 2014;57(4):671–9.
16. Ahadi A, Sun QP. Grain size dependence of fracture toughness and crack-growth resistance of superelastic NiTi. *Scr Mater.* 2016;113:171–5.
17. Brinson LC, Schmidt I, Lammering R. Stress-induced transformation behavior of a polycrystalline NiTi shape memory alloy: micro and macromechanical investigations via in situ optical microscopy. *J Mech Phys Solids.* 2004;52:1549–71.
18. ter Haar D, Wergeland HNS. *Elements of thermodynamics.* Reading: Addison-Wesley Publishing Company; 1966.
19. Gastien R, Corbellani CE, Sade M, Lovey FC. Thermodynamical aspects of martensitic transformations in CuAlNi single crystals. *Scr Mater.* 2004;50(8):1103–7.
20. Gastien R, Corbellani CE, Sade M, Lovey F. A  $\sigma$ -T diagram analysis regarding the  $\gamma'$  inhibition in  $\beta \leftrightarrow \beta' + \gamma'$  cycling in CuAlNi single crystals. *Scr Mater.* 2006;54:1451–5.